

Supplementary Materials for
The maternal microbiome promotes placental development in mice

Geoffrey N. Pronovost *et al.*

Corresponding author: Geoffrey N. Pronovost, geoffpronovost@gmail.com,

Elaine Y. Hsiao, ehsiao@g.ucla.edu

Sci. Adv. **9**, eadk1887 (2023)
DOI: 10.1126/sciadv.adk1887

The PDF file includes:

Fig. S1 to S14

Other Supplementary Material for this manuscript includes the following:

Tables S1 to S5
Data S1 to S18

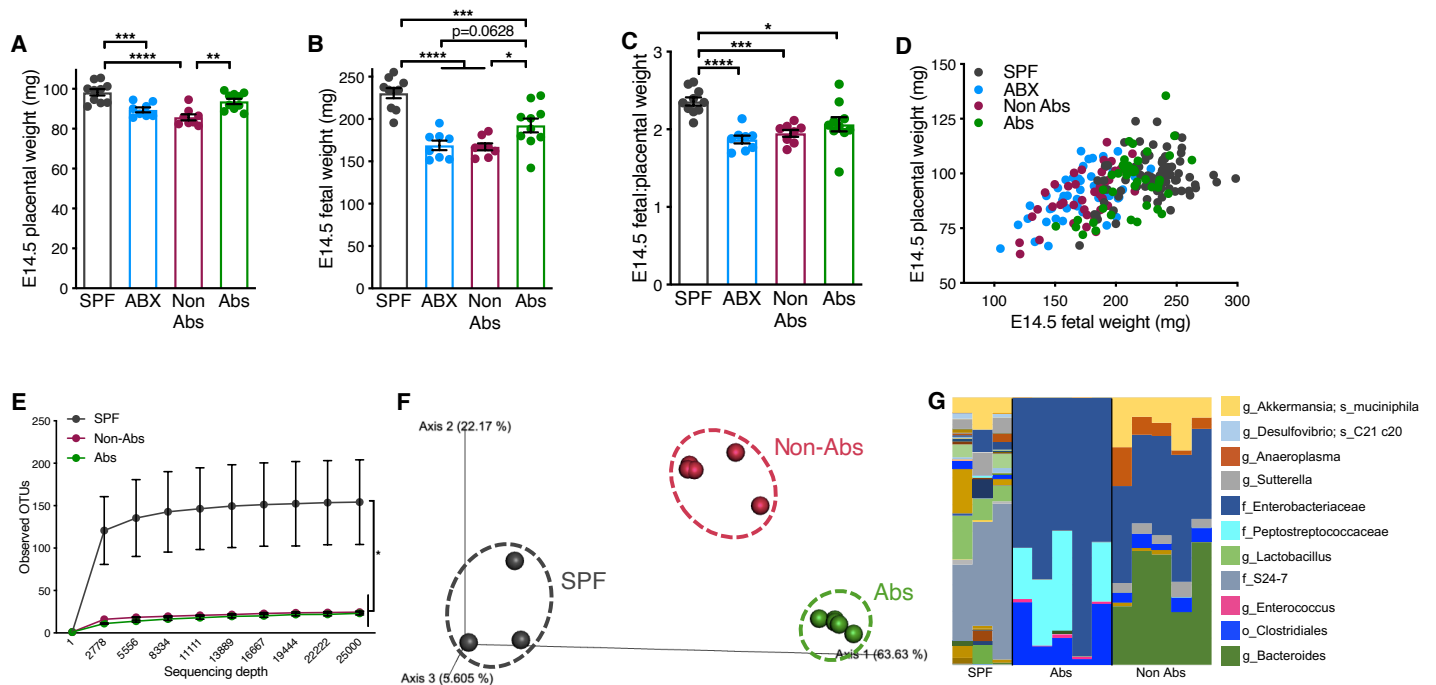


Fig. S1: Antibiotic-induced reductions in placental and fetal weight are not due to off-target effects of absorbable antibiotics. (A) E14.5 placental weights by litter average (SPF ($n = 10$; same as shown in Fig. 1), ABX (ampicillin, metronidazole, neomycin and vancomycin; $n = 9$), Non-absorbable antibiotics (Non-Abs; neomycin and vancomycin; $n = 8$) and absorbable antibiotics (Abs; ampicillin and metronidazole; $n = 10$). (B) E14.5 fetal weights by litter average from litters shown in Fig. S1A. (C) E14.5 fetal to placental weight ratios for litters shown in Fig. S1A-B. (D) Linear correlation of E14.5 placental to fetal weight ratios for all individual conceptuses (SPF ($n = 80$), ABX ($n = 49$), Non-Abs ($n = 40$) and Abs ($n = 42$)) from litters shown in Fig. S1A-C. (E) Alpha-rarefaction curves of 16S rRNA gene sequencing results from E14.5 maternal fecal samples collected from independent cages (SPF ($n = 3$), Non-Abs ($n = 5$) and Abs ($n = 5$)). (F) Weighted UniFrac analysis of 16S rRNA gene sequencing results from E14.5 maternal fecal samples shown in Fig. S1E. (G) Taxa bar plots for 16S rRNA gene sequencing results from E14.5 maternal fecal samples shown in Fig. S1E-F. Data represent mean \pm SEM; statistics were performed with one-way ANOVA with Tukey *post hoc* test. * $P < 0.05$; ** $P < 0.01$; *** $P < 0.001$; **** $P < 0.0001$.

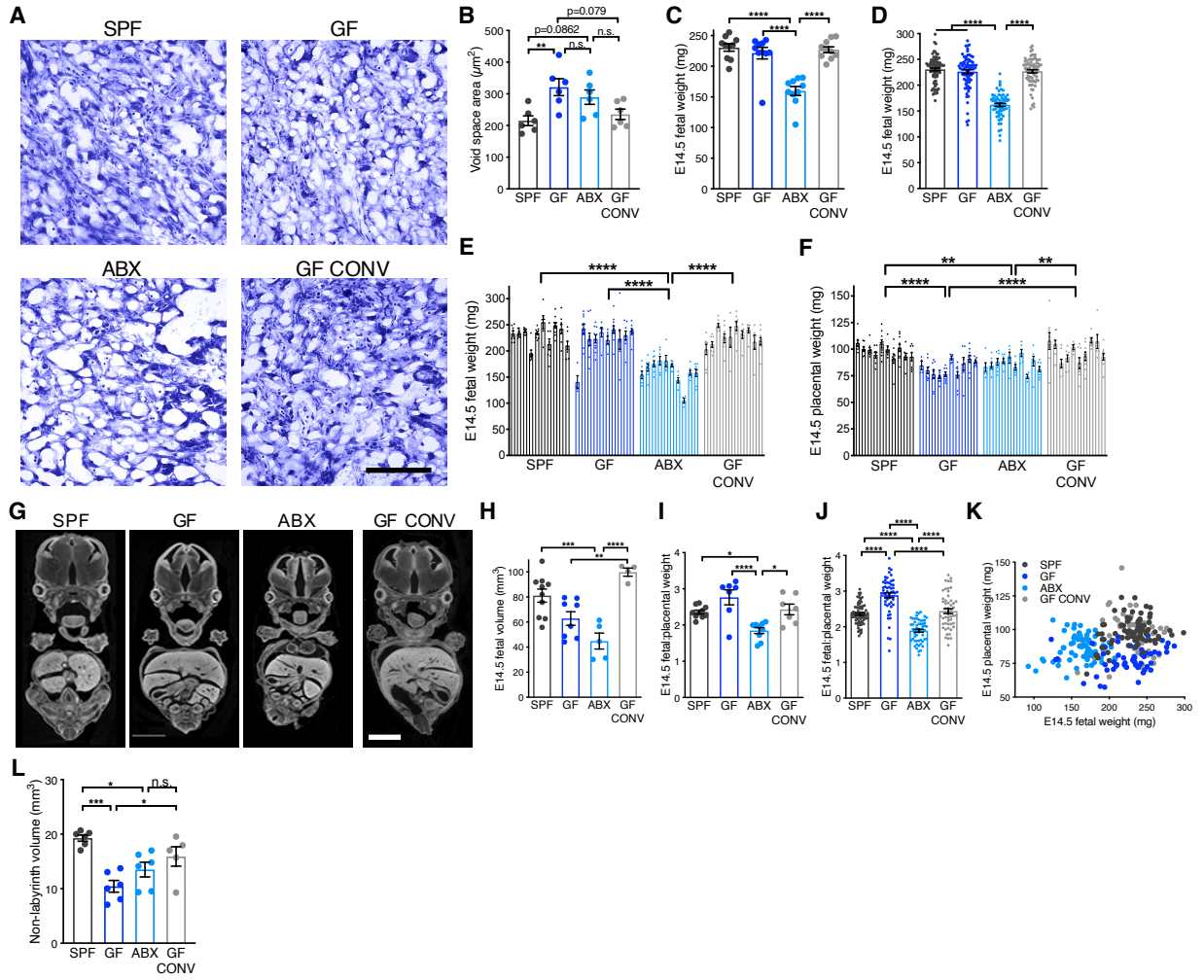


Fig. S2: Maternal microbiome depletion differentially affects E14.5 fetal weight. (A) Representative images of thionin-stained E14.5 placental labyrinth tissues from SPF, GF, ABX and GF CONV litters (scale bar = 250 μm). **(B)** Quantification of average placental labyrinth void space area from litters shown in Fig. S2A (SPF ($n = 6$), GF ($n = 6$), ABX ($n = 6$) and GF CONV ($n = 6$)). **(C)** E14.5 fetal weights by litter average (SPF ($n = 10$), GF ($n = 10$), ABX ($n = 10$) and GF CONV ($n = 10$)). **(D)** E14.5 fetal weights for each individual from litters shown in Fig. S2C (SPF ($n = 80$), GF ($n = 81$), ABX ($n = 65$) and GF CONV ($n = 77$)). **(E)** Individual E14.5 fetal weights used for 1-way nested statistical analysis from litters shown in Fig. S2C (SPF ($n = 80$), GF ($n = 81$), ABX ($n = 65$) and GF CONV ($n = 77$)). **(F)** Individual E14.5 placental weights used for 1-way nested statistical analysis from litters shown in Fig. S2C (SPF ($n = 80$), GF ($n = 81$), ABX ($n = 65$) and GF CONV ($n = 77$)). **(G)** Representative cross-sections of E14.5 whole fetal μCT reconstructions from SPF, GF, ABX and GF CONV litters (scale = 1mm). μCT images in this study are the same as those used for brain volume quantitation in Vuong et al, 2020. **(H)** Quantification of E14.5 whole fetal volumes from μCT reconstructions by litter average (SPF ($n = 10$), GF ($n = 8$), ABX ($n = 5$) and GF CONV ($n = 4$)). **(I)** E14.5 fetal to placental weight ratio for litters shown in Fig. S2C (SPF ($n = 10$), GF ($n = 10$), ABX ($n = 10$) and GF CONV ($n = 10$)). **(J)** E14.5 fetal to placental weight ratios for individual conceptuses from litters shown in Fig. S2G (SPF ($n = 80$), GF ($n = 81$), ABX ($n = 65$) and GF CONV ($n = 77$) litters). **(K)** Linear correlation of E14.5 placental to fetal weight ratios for individual conceptuses shown in Fig. S2H. **(L)** Quantification of E14.5 non-labyrinth placental volumes from μCT reconstructions by litter average (SPF ($n = 6$), GF ($n = 6$), ABX ($n = 6$) and GF CONV ($n = 5$)). Data represent mean \pm SEM; statistics were performed with one-way ANOVA with Tukey *post hoc* test (litter averages) or with 1-way nested with Sidak multiple comparisons correction (individual conceptuses). * $P < 0.05$; ** $P < 0.01$; *** $P < 0.001$; **** $P < 0.0001$.

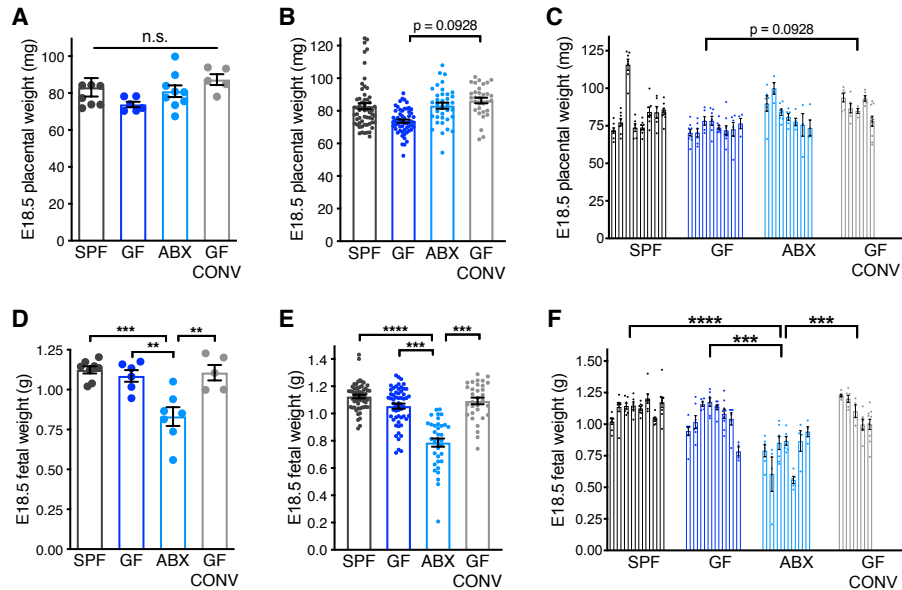


Fig. S3: Maternal microbiome depletion differentially affects E18.5 fetal weight. (A) E18.5 placental weights by litter average (SPF ($n = 7$), GF ($n = 6$), ABX ($n = 9$) and GF CONV ($n = 5$)). (B) E18.5 placental weights for each individual from litters shown in Fig. S3A (SPF ($n = 59$), GF ($n = 56$), ABX ($n = 36$) and GF CONV ($n = 32$)). (C) Individual E18.5 placental weights used for 1-way nested statistical analysis from litters shown in Fig. S3A (SPF ($n = 59$), GF ($n = 56$), ABX ($n = 36$) and GF CONV ($n = 32$)). (D) E18.5 fetal weights by litter average from litters shown in S3A (SPF ($n = 7$), GF ($n = 6$), ABX ($n = 9$) and GF CONV ($n = 5$)). (E) E18.5 fetal weights for each individual from litters shown in Fig. S3A (SPF ($n = 59$), GF ($n = 56$), ABX ($n = 36$) and GF CONV ($n = 32$)). (F) Individual E18.5 fetal weights used for 1-way nested statistical analysis from litters shown in Fig. S3A (SPF ($n = 59$), GF ($n = 56$), ABX ($n = 36$) and GF CONV ($n = 32$)). Data represent mean \pm SEM; statistics were performed with one-way ANOVA with Tukey *post hoc* test (litter averages) or with 1-way nested with Sidak multiple comparisons correction (individual conceptuses). ** $P < 0.01$; *** $P < 0.001$; **** $P < 0.0001$.

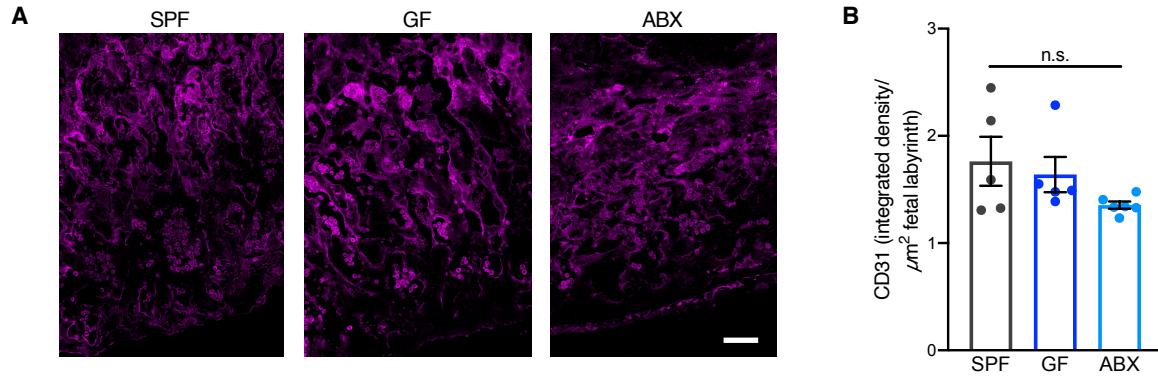


Fig. S4: E10.5 microvasculature density is not affected by maternal microbiota depletion. (A) Representative images of CD31-stained E10.5 placental labyrinth from SPF, GF and ABX (scale bar = 50 μm). (B) Quantification of raw integrated density of CD31 staining intensity, normalized to fetal labyrinth total area (SPF ($n = 5$), GF ($n = 5$) and ABX ($n = 6$)). Data represent mean \pm SEM; statistics were performed with one-way ANOVA with Tukey *post hoc* test.

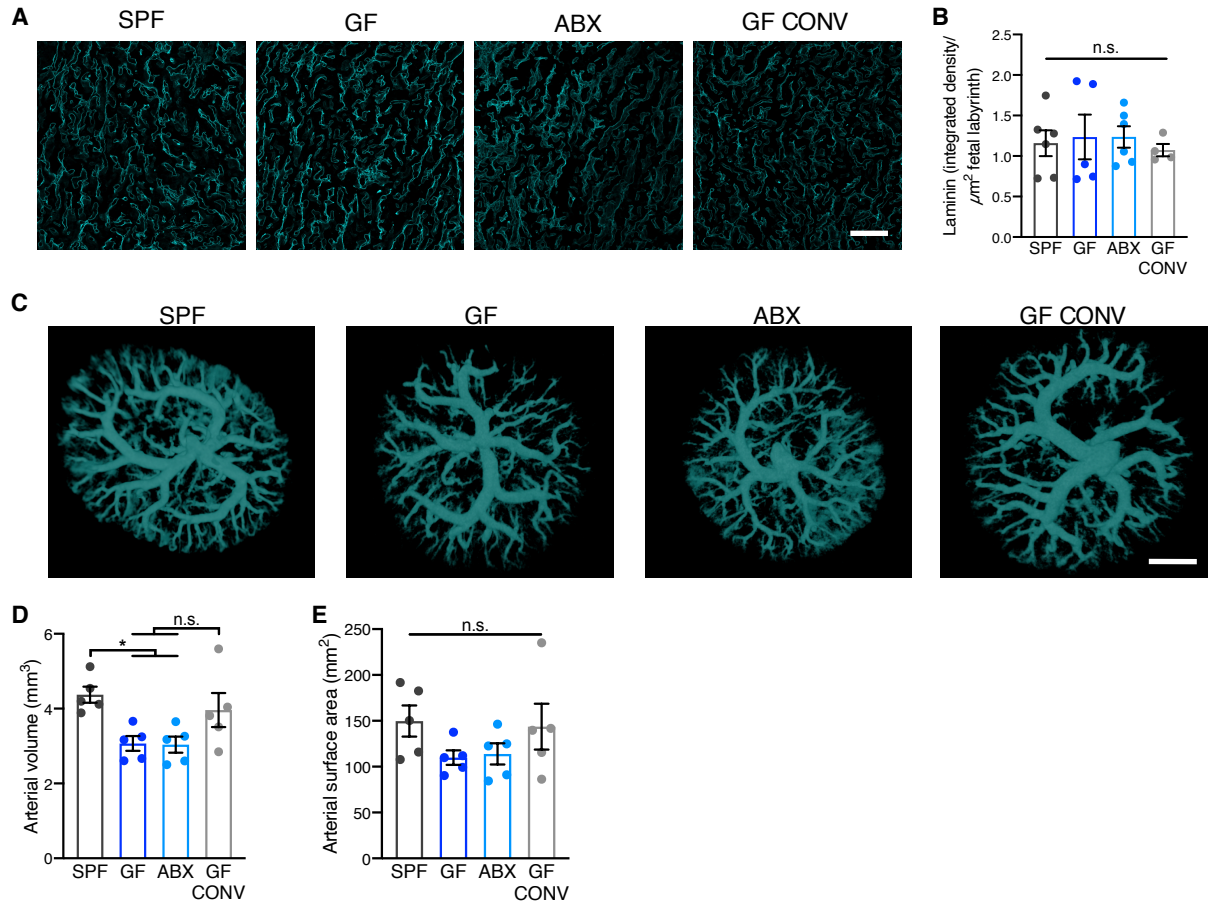


Fig. S5: The maternal microbiome promotes placental vascular development in the late-term placenta. (A) Representative images of laminin-stained E18.5 placental labyrinth from SPF, GF, ABX and GFCONV litters (scale bar = 100 μm). (B) Quantification of raw integrated density of laminin staining intensity, normalized to fetal labyrinth total area (SPF ($n = 6$), GF ($n = 5$), ABX ($n = 5$) and GF CONV ($n = 4$)). (C) Representative fetoplacental arterial vascular reconstructions by μCT imaging of vascular casts from E18.5 SPF, GF, ABX and GF CONV litters; scale bar = 1 mm. (D) Quantification of E18.5 fetoplacental arterial vascular volume (SPF ($n = 5$), GF ($n = 5$), ABX ($n = 5$) and GF CONV ($n = 5$)). (E) Quantification of E18.5 fetoplacental arterial vascular surface area (SPF ($n = 5$), GF ($n = 5$), ABX ($n = 5$) and GF CONV ($n = 5$)). Data represent mean \pm SEM; statistics were performed with one-way ANOVA with Tukey *post hoc* test. * $P < 0.05$.

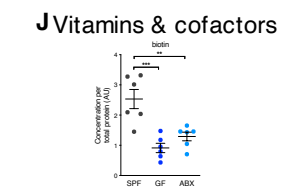
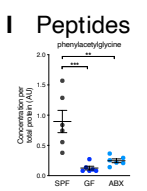
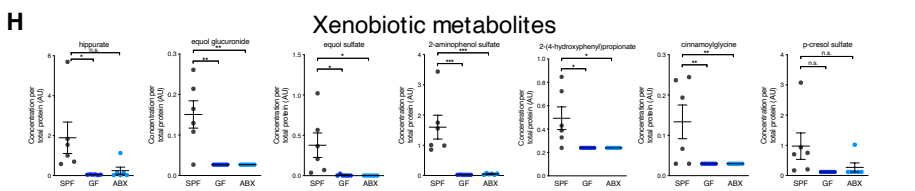
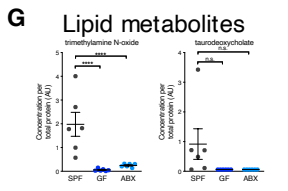
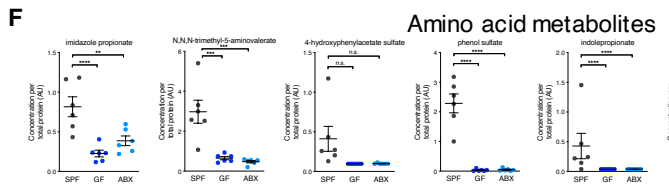
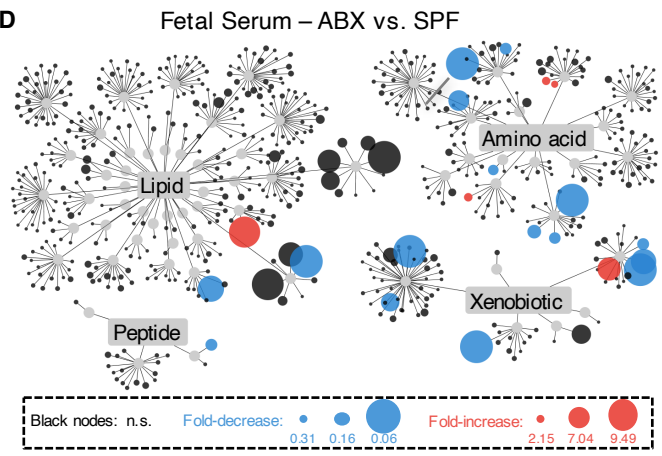
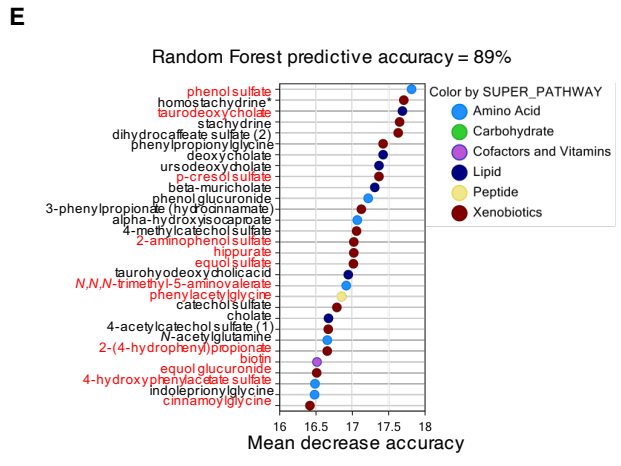
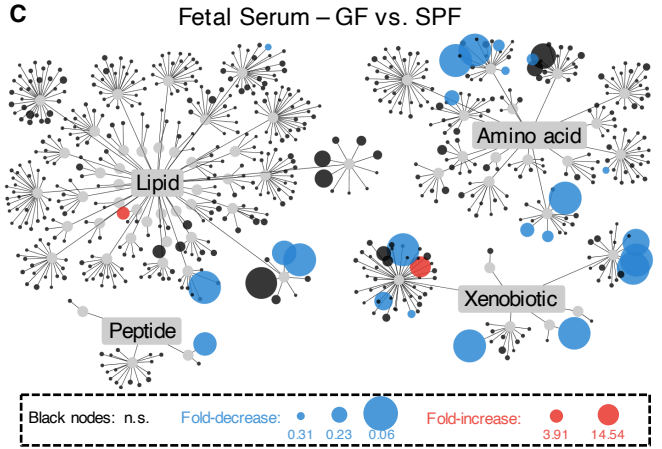
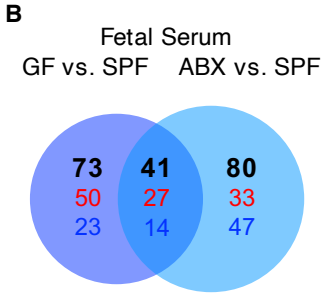
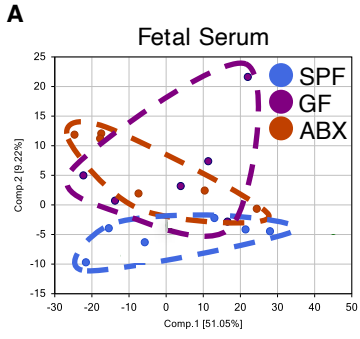


Fig. S6: The maternal microbiome modulates the fetal serum metabolome. (A) Principal component analyses of E14.5 fetal serum (SPF ($n = 6$), GF ($n = 6$) and ABX ($n = 6$)). (B) Significantly altered metabolites (black text), both downregulated (red text) and upregulated (blue text) in litters represented in Fig. S3B. (C) Global metabolite profile changes in GF fetal serum relative to SPF fetal serum. (D) Global metabolite profile changes in ABX fetal serum relative to SPF fetal serum. (E) Random Forest analysis (predictive accuracy of 89%) identifying the top 30 fetal serum metabolites that distinguish samples as GF or ABX, relative to SPF (metabolites used for *in vivo* supplementation labeled with red text). (F) Relative concentrations of amino acid metabolites used for *in vivo* metabolite supplementation from litters represented in Fig. S3A-B. (G) Relative concentrations of lipid metabolites used for *in vivo* metabolite supplementation from litters represented in Fig. S3A-B. (H) Relative concentrations of xenobiotic metabolites used for *in vivo* metabolite supplementation from litters represented in Fig. S3A-B. (I) Relative concentration of peptide metabolites used for *in vivo* metabolite supplementation from litters represented in Fig. S3A-B. (J) Relative concentration of vitamin & cofactor metabolites used for *in vivo* metabolite supplementation from litters represented in Fig. S3A-B. Statistical comparisons for all but Fig. S7A and S7E are based on unadjusted $P < 0.05$. Data represent mean \pm SEM; statistics were performed with one-way ANOVA with Tukey *post hoc* test. * $P < 0.05$; ** $P < 0.01$; *** $P < 0.001$; **** $P < 0.0001$.

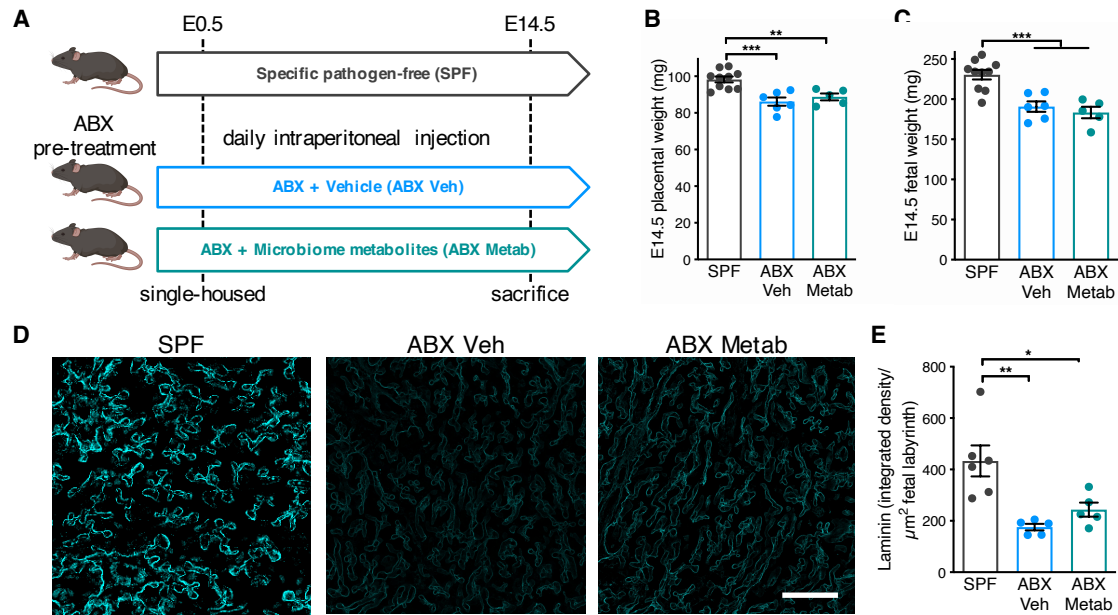


Fig. S7: Select microbiome-dependent metabolites do not rescue placental growth and vascular impairments induced by maternal microbiome depletion. (A) Schematic for microbiome-dependent metabolite supplementation in ABX mice. (B) E14.5 placental weights by litter average (SPF ($n = 10$; same as shown in Fig. 1A), ABX Veh ($n = 6$) and ABX Metab ($n = 5$)). (C) E14.5 fetal weights for litter averages shown in Fig. S4B. (D) Representative images of laminin-stained E14.5 placental labyrinth from SPF (same as in Fig. 2A), ABX Veh and ABX Metab litters. (E) Quantification of raw integrated density of laminin intensity, normalized to fetal labyrinth total area (SPF ($n = 6$; same as shown in Fig. 2C), ABX Veh ($n = 5$) and ABX Metab ($n = 5$)). Data represent mean \pm SEM; statistics were performed with one-way ANOVA with Tukey *post hoc* test. * $P < 0.05$; ** $P < 0.01$; *** $P < 0.001$.

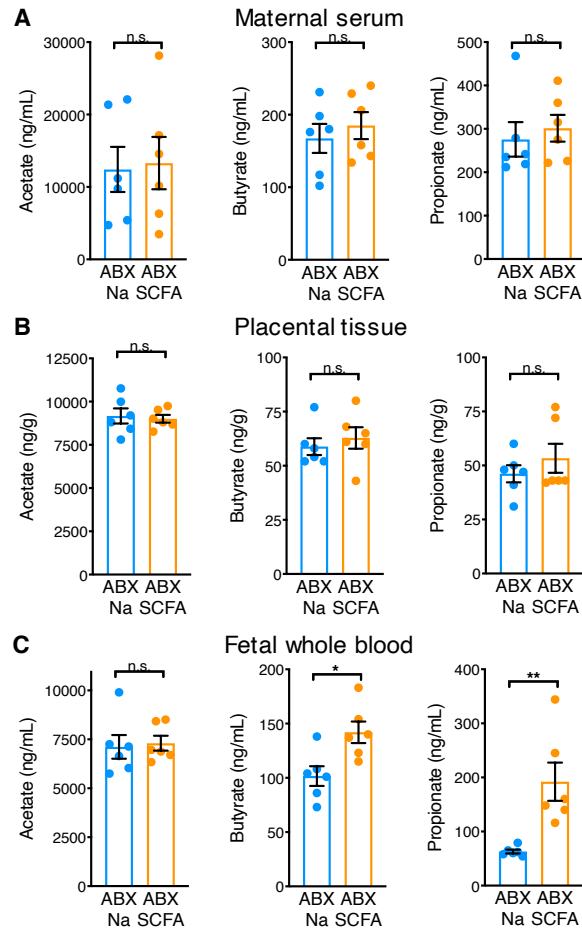


Fig. S8: Intra-gastric SCFA administration increases fetal blood butyrate and propionate in ABX-treated dams. (A) Quantification of E14.5 maternal serum acetate, butyrate and propionate concentrations, respectively (ABX Na ($n = 6$) and ABX SCFA ($n = 6$)). (B) Quantification of E14.5 whole placental tissue acetate, butyrate and propionate concentrations, respectively (ABX Na ($n = 6$) and ABX SCFA ($n = 6$)). (C) Quantification of E14.5 fetal whole blood acetate, butyrate and propionate concentrations, respectively (ABX Na ($n = 6$) and ABX SCFA ($n = 6$)). Data represent mean \pm SEM; statistics were performed with student's t test with Tukey *post hoc* test. * $P < 0.05$; ** $P < 0.01$.

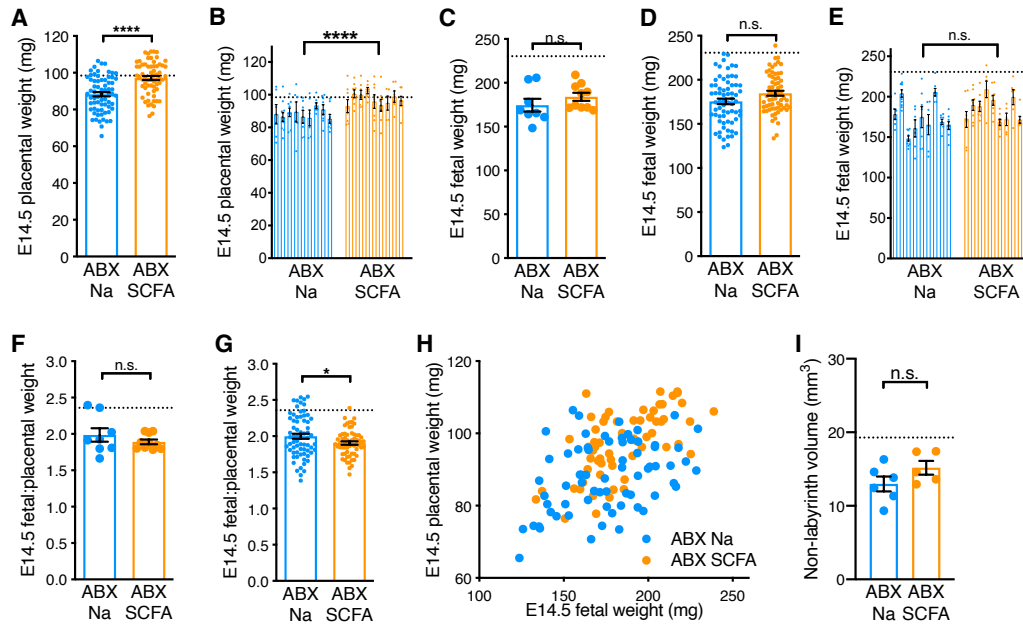


Fig. S9: SCFA supplementation does not alter E14.5 fetal growth in microbiota-depleted dams. (A) E14.5 placental weights for each individual from litters shown in Fig. 3A (ABX Na ($n = 68$) and ABX SCFA ($n = 63$); hashed line represents SPF litter average value shown in Fig. 1B). (B) Individual E14.5 placental weights used for 1-way nested statistical analysis from litters shown in Fig. S5A (ABX Na ($n = 68$) and ABX SCFA ($n = 63$)). (C) E14.5 fetal weights by litter average for litters shown in Fig. S5A (hashed line represents SPF litter average value shown in Fig. S2B). (D) E14.5 fetal weights for each individual from litters shown in Fig. S5A (hashed line represents SPF litter average value shown in Fig. S2C). (E) Individual E14.5 fetal weights used for 1-way nested statistical analysis from litters shown in Fig. S5A (ABX Na ($n = 68$) and ABX SCFA ($n = 63$)). (F) E14.5 fetal to placental weight ratios by litter average for litters shown in Fig. S5A-C (hashed line represents SPF litter average value shown in Fig. S2F). (G) E14.5 individual fetal to placental weight ratios from litters shown in Fig. S5D (hashed line represents SPF litter average value shown in Fig. S2G). (H) Linear correlation of E14.5 placental to fetal weight ratios for individual conceptuses shown in Fig. S5A-C. (I) Quantification of E14.5 non-labyrinth placental volumes from μ CT reconstructions by litter average (ABX Na ($n = 6$) and ABX SCFA ($n = 5$); hashed line represents SPF litter average value shown in Fig. S3L). Means \pm SEM (error bars) plotted; statistics were performed with student's t test (litter averages) or with 1-way nested with Sidak multiple comparisons correction (individual conceptuses). . * $P < 0.05$; **** $P < 0.0001$.

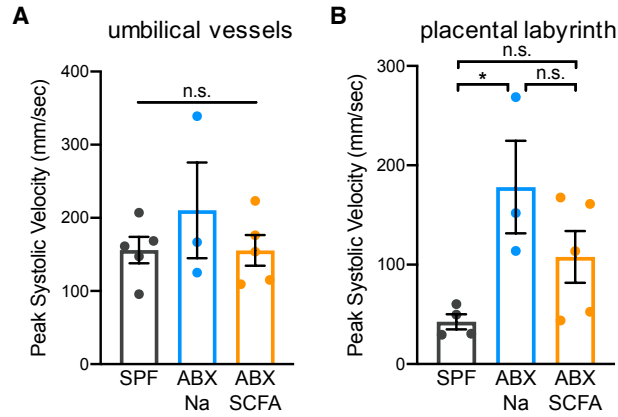


Fig. S10: Maternal SCFA administration partially alleviates impairments in placental labyrinth vascular flow induced by maternal microbiome depletion. (A) Quantification of E14.5 peak systolic velocity in umbilical vessels (SPF ($n = 5$), ABX Na ($n = 3$) and ABX SCFA ($n = 5$)). (B) Quantification of E14.5 peak systolic velocity in placental labyrinth from litters shown in SXA (SPF ($n = 5$), ABX Na ($n = 3$) and ABX SCFA ($n = 5$)). Data represent mean \pm SEM; statistics were performed with one-way ANOVA with Tukey *post hoc* test. * $P < 0.05$.

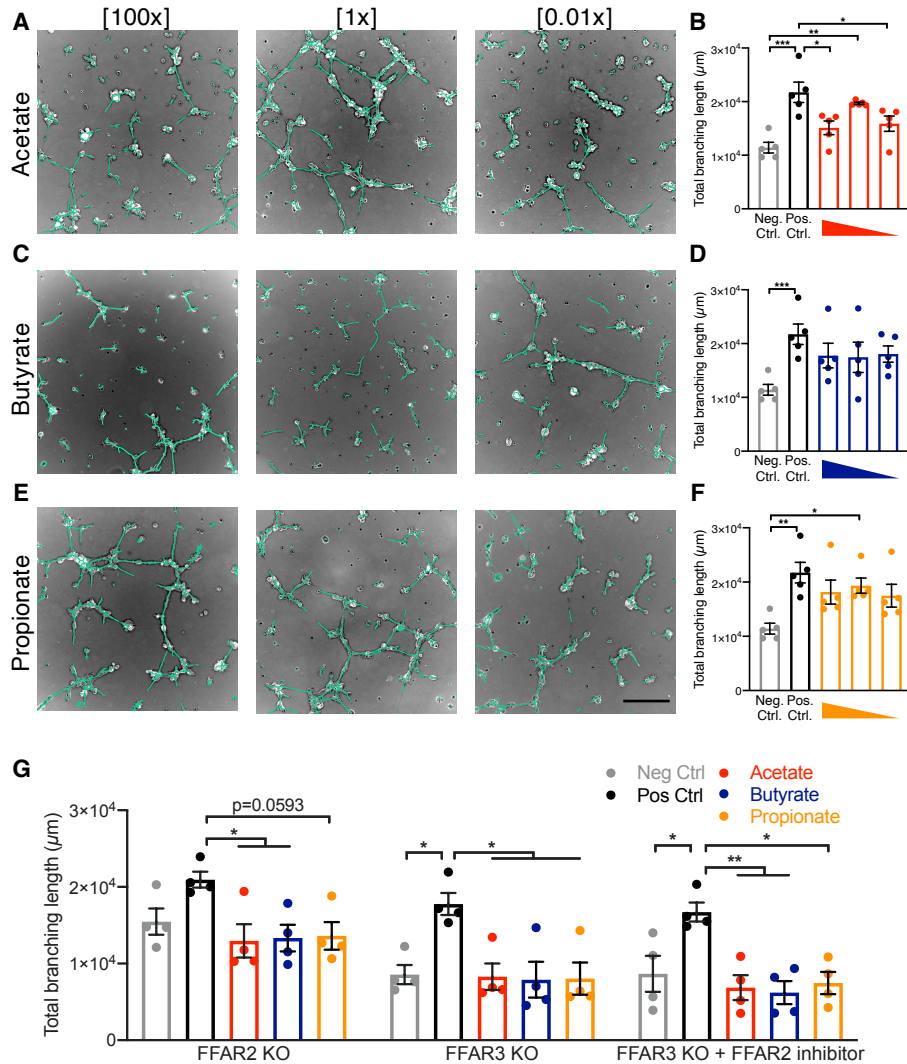


Fig. S11: SCFAs promote HUVEC tube formation *in vitro*. (A) Representative images for HUVECs treated with 4 mM, 40 μM and 0.4 μM acetate, respectively. (B) Quantification of acetate-supplemented HUVEC tube formation assays. (C) Representative images for HUVECs treated with 500 μM , 5 μM and 0.05 μM butyrate, respectively. (D) Quantification of propionate-supplemented HUVEC tube formation assays. (E) Representative images for HUVECs treated with 500 μM , 5 μM and 0.05 μM propionate, respectively. (F) Quantification of butyrate-supplemented HUVEC tube formation assays. (G) Quantification of tube formation assays from FFAR2KO HUVECs, FFAR3KO HUVECs and FFAR3KO + FFAR2 inhibitor-treated HUVECs, respectively, treated with 40 μM acetate, 5 μM butyrate or 5 μM propionate. Scale bar = 250 μm . Data represent mean \pm SEM; statistics were performed with one-way ANOVA with Tukey *post hoc* test. * $P < 0.05$; ** $P < 0.01$; *** $P < 0.001$.

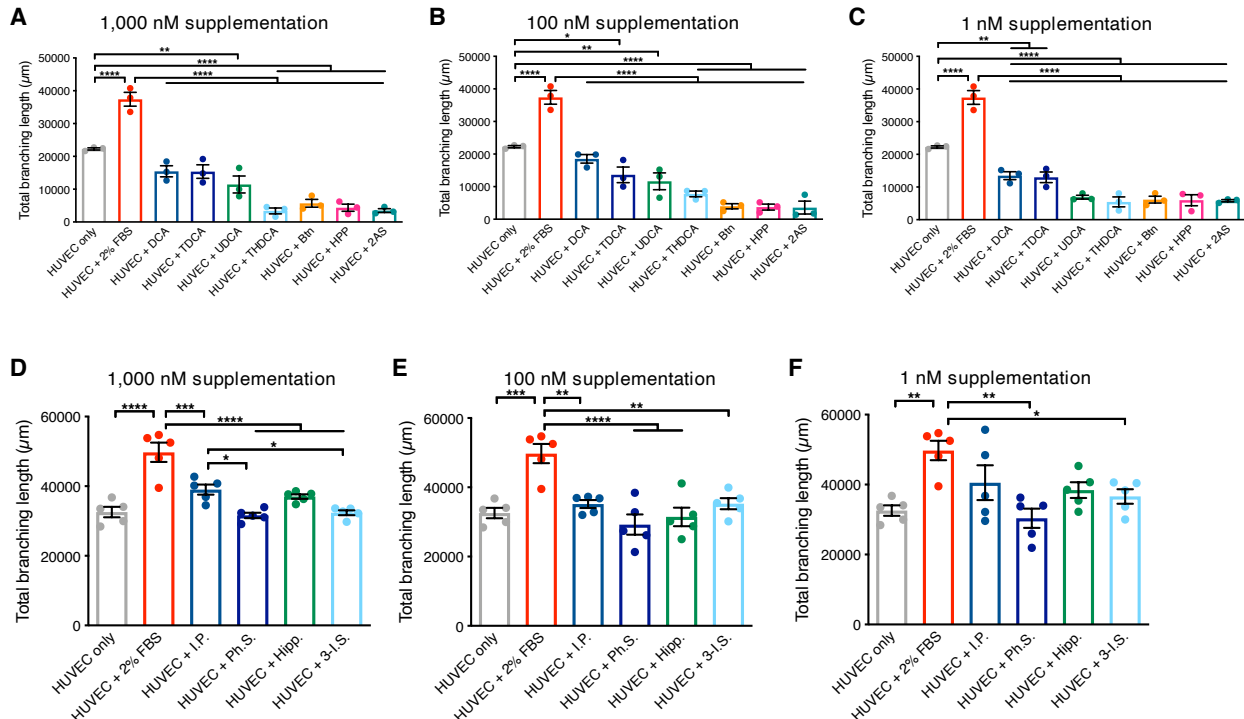


Fig. S12: Select microbiome-dependent metabolites do not promote HUVEC tube formation *in vitro*. (A) Quantification of HUVEC branching length in non-supplemented media (HUVEC only, negative control), 2% FBS-supplemented media (positive control), and supplementation with 1,000 nM deoxycholate (DCA), taurodeoxycholate (TDCA), ursodeoxycholate (UDCA), taurohyodeoxycholate (THDCA), biotin (Btn), 2-(4-hydroxyphenyl)propionate (HPP) and 2-aminophenol sulfate (2AS), respectively. (B) Quantification of HUVEC branching length in non-supplemented media, 2% FBS-supplemented media, and supplementation with 100 nM DCA, TDCA, UDCA, THDCA, Btn, HPP and 2AS, respectively. (C) Quantification of HUVEC branching length in non-supplemented media, 2% FBS-supplemented media, and supplementation with 1 nM DCA, TDCA, UDCA, THDCA, Btn, HPP and 2AS, respectively. (D) Quantification of HUVEC branching length in non-supplemented media, 2% FBS-supplemented media, and supplementation with 1,000 nM imidazole propionate (I.P.), phenol sulfate (Ph.S.), hippurate (Hipp.) and 3-indoxyl sulfate (3-I.S.), respectively. (E) Quantification of HUVEC branching length in non-supplemented media, 2% FBS-supplemented media, and supplementation with 100 nM imidazole propionate (I.P.), phenol sulfate (Ph.S.), hippurate (Hipp.) and 3-indoxyl sulfate (3-I.S.), respectively. (F) Quantification of HUVEC branching length in non-supplemented media, 2% FBS-supplemented media, and supplementation with 1 nM imidazole propionate (I.P.), phenol sulfate (Ph.S.), hippurate (Hipp.) and 3-indoxyl sulfate (3-I.S.), respectively. Data represent mean \pm SEM; statistics were performed with one-way ANOVA with Tukey *post hoc* test. * $P < 0.05$; ** $P < 0.01$; *** $P < 0.001$; **** $P < 0.0001$.

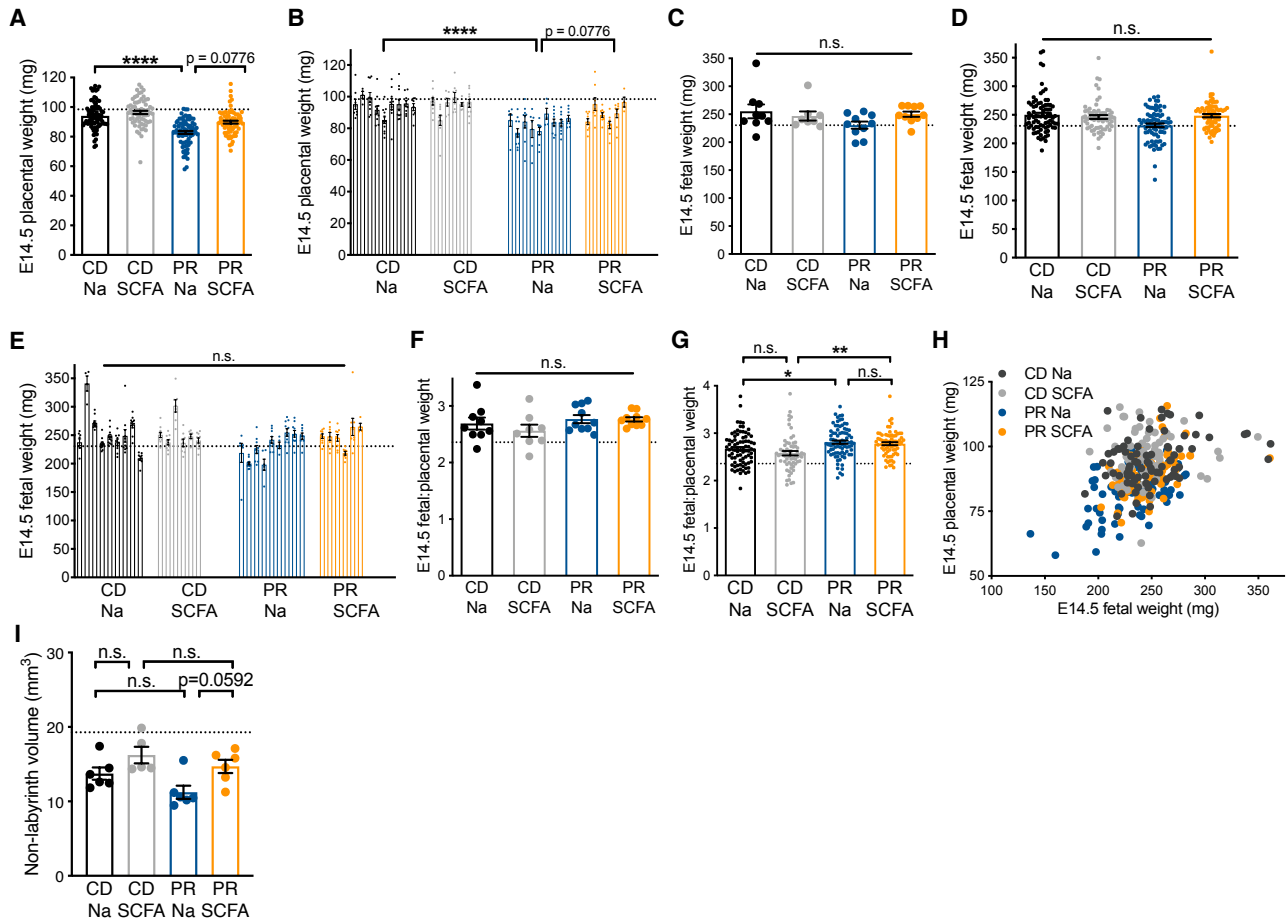


Fig. S13: Maternal SCFA supplementation modestly increases E14.5 fetal growth in protein-restricted dams. (A) E14.5 placental weights for each individual from litters shown in Fig. 4A (CD Na ($n = 80$), CD SCFA ($n = 65$), PR Na ($n = 81$) and PR SCFA ($n = 72$); hashed line represents SPF litter average value shown in Fig. 1B). (B) Individual E14.5 placental weights used for 1-way nested statistical analysis from litters shown in Fig. S8A (CD Na ($n = 80$), CD SCFA ($n = 65$), PR Na ($n = 81$) and PR SCFA ($n = 72$)). (C) E14.5 fetal weights by litter average for litters shown in Fig. S8A (hashed line represents SPF litter average value shown in Fig. S2B). (D) E14.5 fetal weights for each individual from litters shown in Fig. S8A (hashed line represents SPF litter average value shown in Fig. S2C). (E) Individual E14.5 fetal weights used for 1-way nested statistical analysis from litters shown in Fig. S8D (CD Na ($n = 80$), CD SCFA ($n = 65$), PR Na ($n = 81$) and PR SCFA ($n = 72$)). (F) E14.5 fetal to placental weight ratios by litter average for litters shown in Fig. S5A-C (hashed line represents SPF litter average value shown in Fig. S2F). (G) E14.5 individual fetal to placental weight ratios from litters shown in Fig. S5D (hashed line represents SPF litter average value shown in Fig. S2G). (H) Linear correlation of E14.5 placental to fetal weight ratios for individual conceptuses shown in Fig. S5A-C. (I) Quantification of E14.5 non-labyrinth placental volumes from μ CT reconstructions by litter average (CD Na ($n = 6$), CD SCFA ($n = 5$), PR Na ($n = 6$) and PR SCFA ($n = 5$); hashed line represents SPF litter average value shown in Fig. S3L). Data represent mean \pm SEM; statistics were performed with two-way ANOVA with Tukey *post hoc* test (litter averages) or with 1-way nested with Sidak multiple comparisons correction (individual conceptuses). ** $P < 0.01$; **** $P < 0.0001$.

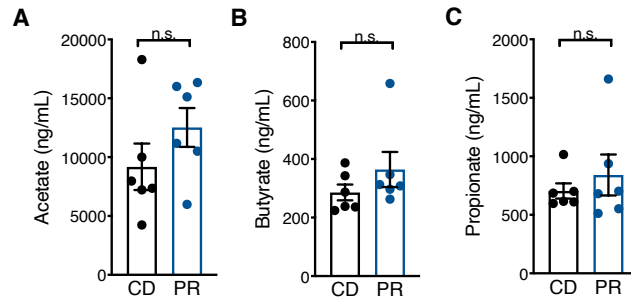


Fig. S14: Maternal serum SCFA concentrations are not affected in dietary maternal protein restriction model. (A) Quantification of E18.5 maternal serum acetate concentrations (CD ($n = 6$) and PR ($n = 6$)). **(B)** Quantification of E18.5 maternal serum butyrate concentrations (CD ($n = 6$) and PR ($n = 6$)). **(C)** Quantification of E18.5 maternal serum propionate concentrations (CD ($n = 6$) and PR ($n = 6$)). Data represent mean \pm SEM; statistics were performed with student's t test with Tukey *post hoc* test.

Table S1 (separate file): Metabolites in E14.5 SPF, GF and ABX fetal blood

Table S2 (separate file): Metabolites used for in vivo supplementation in ABX dams

Table S3 (separate file): Metabolite concentrations used in HUVEC branching tube formation assays

Table S4 (separate file): 16S rRNA gene sequencing of fecal microbiota from ABX, Non Abs and Abs dams on E14.5

Table S5 (separate file): Compositions of mouse diets

Data S1 to S18 (separate file): Raw input data for each graph of all figures.